Ultrasonics 98 (2019) 94–98

Contents lists available at ScienceDirect

Ultrasonics

journal homepage: www.elsevier.com/locate/ultras

Non-invasive photoacoustic detection of hidden underdrawings in paintings using air-coupled transducers

George J. Tserevelakis*, Panagiotis Siozos, Athanasia Papanikolaou, Kristalia Melessanaki, Giannis Zacharakis

Foundation for Research and Technology Hellas, Institute of Electronic Structure and Laser, N. Plastira 100, Heraklion, Crete GR-70013, Greece

ARTICLE INFO

Keywords:
Photoacoustic imaging
Cultural heritage
Art conservation
Paintings
Non-destructive
Non-invasive

ABSTRACT

We demonstrate the application of a fully non-contact and non-invasive photoacoustic (PA) imaging system integrating a high sensitivity spherically focused air-coupled ultrasonic transducer, for the uncovering of hidden underdrawings in paintings. By selectively transforming optical absorption information into ultrasonic waves which propagate virtually unobstructed through the paint layers, PA signals provide specific imaging of underlying pencil sketches even for paints presenting high optical scattering and absorption properties. The developed system could be employed for case studies involving the investigation of paintings with historical significance, considerably complementing the capabilities of existing methods.

1. Introduction

Paintings typically consist of several successive turbid layers of paint demonstrating strong optical scattering and absorption properties arising mainly from the pigment particles. As a result, pure optical imaging methods are rather limited to a superficial investigation of the artwork and thus hidden features including underdrawings and underpaintings, which have been painted over, may escape detection. The non-destructive recovery of such hidden information could shed light to the historical, social, geographical or even psychological framework of the artistic creation, providing valuable knowledge not only to art historians, but also to conservation scientists who are interested in the verification of artworks' authenticity [1,2].

To overcome the limitations of optical diagnostic methods in cultural heritage (CH), a novel photoacoustic (PA) imaging approach was recently assessed as regards to the accurate in-depth extraction of invisible information in artworks. PA imaging is based on the formation of acoustic waves following the absorption of intensity-modulated (typically pulsed) optical radiation by a material [3]. In particular, a portion of the absorbed optical energy is converted into heat, which subsequently causes a rapid thermoelastic expansion and the generation of an initial pressure propagating in space in the form of ultrasonic waves [4,5]. These waves can then be recorded using the same detection equipment (e.g. piezoelectric elements) as in traditional ultrasound imaging. The amplitude of PA waves is directly proportional to the absorption coefficient of the medium for the employed excitation wavelength; therefore, the technique provides optical absorption imaging contrast with high sensitivity.

The high transmissivity of PA waves, as well as, the excellent optical absorption contrast features of PA imaging have successfully permitted the investigation of several opaque CH objects such as paintings and documents [6–8]. However, all these previous proof of concept studies have been using immersion ultrasonic transducers and respective coupling media such as gels and distilled water in direct contact with artwork's surface for the efficient propagation and subsequent detection of the generated PA signals. In order to compete existing diagnostic methods routinely used in CH applications such as infrared imaging, OCT or X-rays [9–11], the PA technique has to be totally non-contact and non-invasive so that it will not threaten, in any case, the integrity of an invaluable work of art. It is clear that under such conditions, PA imaging could be easily incorporated in the diagnostic toolbox of conservation scientists as a simple, reliable, low cost and robust method for the analytical investigation of artworks.

Herewith, we present the application of a fully non-contact PA imaging system customized for CH diagnostics, integrating a high sensitivity spherically focused air-coupled ultrasonic transducer, for the uncovering of hidden features in paintings. To demonstrate the capabilities of the developed system, painting samples were prepared with the aim to replicate real easel paintings in a small scale. It has been shown that the inherent hybrid nature of PA imaging can overcome several major limitations of pure optical diagnostic techniques employed for this purpose, as a consequence of the high transmission of

* Corresponding author.
E-mail address: tserevel@iesl.forth.gr (G.J. Tserevelakis).

https://doi.org/10.1016/j.ultras.2019.06.008
Received 29 January 2019; Received in revised form 26 April 2019; Accepted 11 June 2019
Available online 12 June 2019
0041-624X/

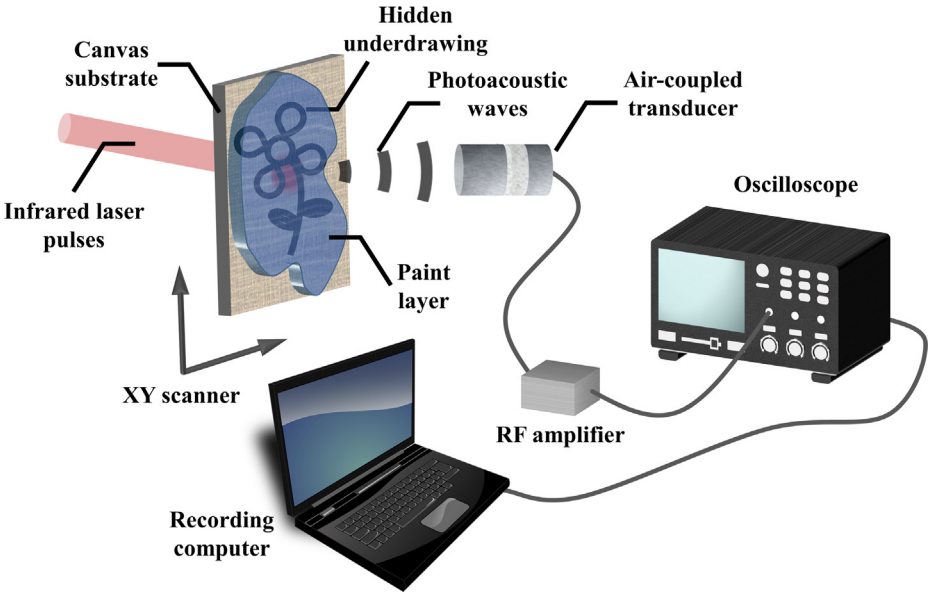

Fig. 1. Schematic representation of the non-contact PA imaging apparatus for the detection of underdrawings in paintings.

the photo-induced acoustic waves through common art media such as paints, acrylic layers, etc.

2. Materials and methods

Various geometric patterns and drawings were produced on the prepared canvas coated with a thin layer of titanium white paint, using a graphite pencil (CASTELL 9000 3B, Faber-Castell, Stein, Germany), representing the hidden underdrawings of the artwork. Subsequently, four characteristic types of pigments, namely, Ultramarine Blue ($Na_7Al_6Si_6O_{24}S_3$, Kremer 4503), Chromium Green (Cr_2O_3, Kremer 44200), Vermillion (HgS, Sigma Aldrich, FLUKA) and Zinc White (ZnO, Kremer 46300) were individually mixed with an acrylic binder (Lascaux Acrylic Adhesive 498 HV) to form thick acrylic paints. Each paint paste was applied with the use of a spatula over the sketches, forming paint layers with a thickness between 0.5 and 2.0 mm.

The non-contact imaging apparatus (Fig. 1) employs a Q-switched Nd:YAG laser (SL404, Spectron Laser Systems, Rugby, England; maximum pulse energy 30 mJ, pulse duration: 10 ns, pulse repetition rate: 10 Hz) emitting infrared radiation at 1064 nm for the efficient excitation of PA signals. The beam is initially attenuated and reduced in diameter to 2 mm using an adjustable iris diaphragm, so that the pulse energy at the surface of the painting sample is less than 4.5 mJ, corresponding to a maximum energy fluence value in the order of 140 mJ/cm^2. Each sample is firmly fixed on a custom-made holder and irradiated from its back surface to generate PA waves from the hidden sketch regions, which are partially transmitted through the overlying paint layer and ambient air prior their detection by the focused non-contact transducer (NCT1-D7-P10, The Ultran Group, State College, PA, USA; nominal central frequency: 1 MHz; focal distance: 10 mm; numerical aperture: 0.31). The signals are subsequently enhanced by two low-noise RF amplifiers (TB-414-8A+, Mini-Circuits, Camberley, England; gain: 31 dB) connected in series to achieve a total gain of 62 dB, which is adequate for the digitization and recording of PA waveforms by an oscilloscope (DSO7034A, Agilent Technologies, Santa Clara, CA, USA; bandwidth: 350 MHz; sample rate: 2 GSa/s). To form an image, the painting is raster scanned along its surface using a set of high precision XY motorized stages (8MTF-75LS05, Standa, Vilinius, Lithuania), to attain a point by point data acquisition in synchronization with the trigger signal of the laser source. The recorded waveforms are averaged two times for signal to noise ratio (SNR) improvement, transferred to a computer and bandpassed between 100 kHz and 2 MHz for high frequency noise elimination before the estimation of the peak-to-peak PA amplitude value providing the contrast of the final 8-bit images.

Depending on the extent of the underlying sketch, the scanning area has been 25 × 25 or 30 × 30 mm^2 respectively, and have been sampled, in both cases, using 100 × 100 pixels. The total time required per imaging session for these scanning parameters has been approximately equal to 45 min.

3. Results and discussion

Prior the underdrawings visualization, we performed a characterization of the employed air-coupled transducer through the detection of PA signals arising from a 170 μm diameter pencil spot on canvas substrate, behaving as an approximately point-like absorber compared to the theoretically predicted diffraction limited acoustic focus (~790 μm) [3]. The time-domain PA signal arising from the pencil spot is shown in Fig. 2a, following the averaging of 16 waveforms within a temporal window of 20 μs. The corresponding normalized amplitude spectrum (Fig. 2b) reveals a central frequency of around 980 kHz, which is in excellent agreement with the nominal transducer's value (error: ~2%). Furthermore, the −6 dB bandwidth has been estimated at 610 kHz, yielding a predicted axial resolution of 500 μm, whereas the respective depth of focus is expected to be around 8.6 mm [3]. On the other hand, the point spread function (PSF) of the imaging system was estimated by raster scanning the pencil spot region over transducer's focus using a pixel size of 60 μm (Fig. 2c). A profile of the measured PSF is explicitly presented in Fig. 2d, where the black line corresponds to a Gaussian fitting of the experimental data ($R^2 > 0.99$). The fitted curve provides a full width at half maximum (FWHM) value approximately equal to 800 μm, which is practically identical to the diffraction limited focal spot of the transducer.

Furthermore, we proceeded to an initial evaluation of the PA signal amplitude arising from graphite regions representing the hidden underdrawings, as well as, the background signals generated from various acrylic paint layers covering the specimens under investigation. Typical PA waveforms acquired at identical conditions from different media are presented explicitly in Fig. 3, demonstrating various peak-to-peak amplitude values which depend directly on the optical absorption magnitude of laser's radiation.

More specifically, graphite generates the highest PA amplitude (66 mV), whereas Zinc White paint layer provides the lowest one

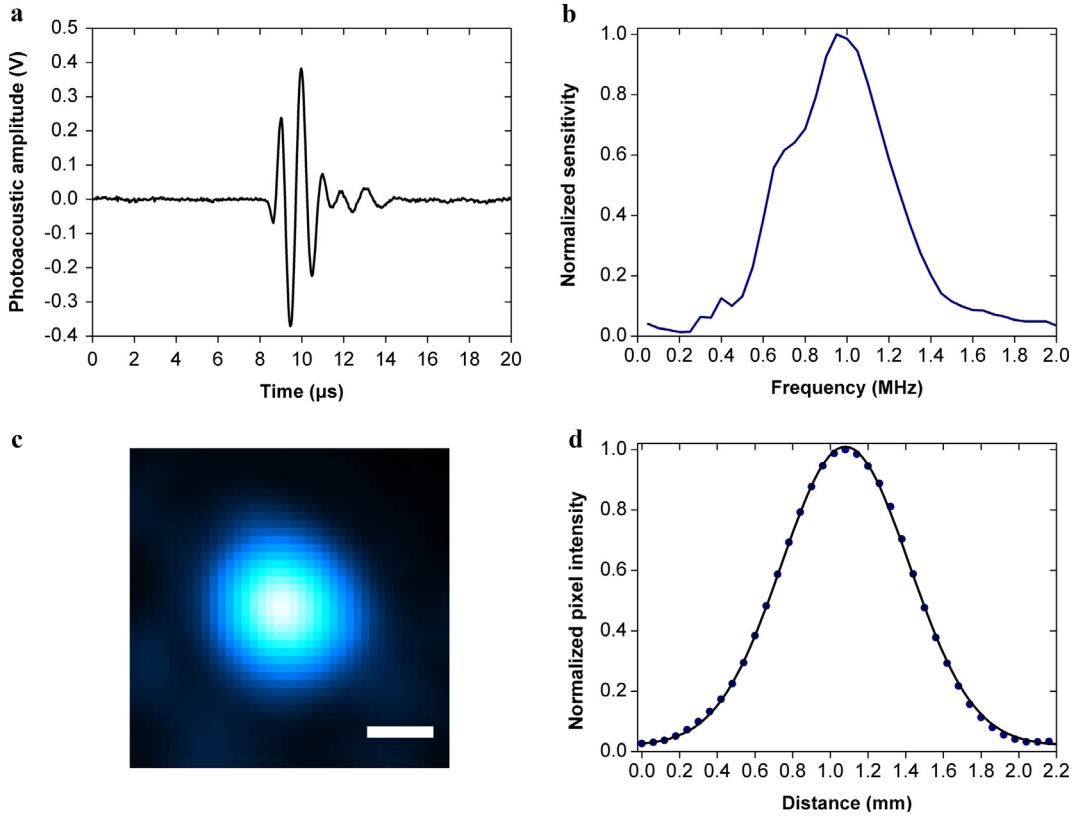

Fig. 2. Characterization of the employed air-coupled ultrasonic transducer by means of PA signal detection. (a) Time-domain PA signal arising from a 170 μm diameter pencil spot on canvas substrate. (b) Normalized amplitude spectrum of the recorded PA waveform. (c) Estimated PSF through the imaging of the pencil spot behaving as an approximately point-like PA signal source. Scalebar: 0.5 mm. (d) PSF profile fitted with a Gaussian curve ($R^2 > 0.99$).

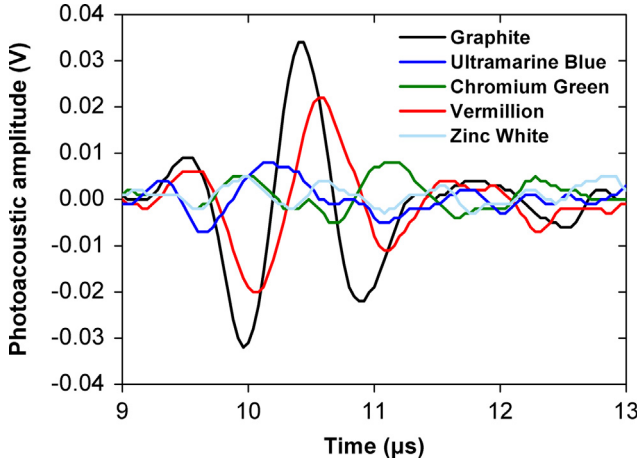

Fig. 3. PA waveforms generated from hidden graphite regions and various acrylic paint layers.

(7 mV). On the other hand, Vermillion, Chromium Green and Ultramarine Blue paint layers present intermediate values of 42, 13 and 15 mV respectively. The imaging contrast C for each case can be estimated by the formula

$$C = \frac{A_{graph} - A_{paint}}{A_{graph} + A_{paint}}$$

where A_{graph} and A_{paint} are the peak-to-peak PA amplitudes for graphite and the overlying paint layer respectively. The highest predicted contrast value is for Zinc White paint layer sample (C = 0.81), whereas the lowest one is for Vermillion layer (C = 0.22), as a result of its appreciable optical absorption properties. High contrast values are additionally calculated for the cases of Chromium Green (C = 0.67) and Ultramarine Blue (C = 0.63) paints, indicating the potential of PA signal regarding the precise discrimination of hidden sketches.

Having accomplished a concise investigation on the performance of the non-contact PA imaging system, we proceeded to the visualization of underdrawings in four samples covered with representative paint layers typically met in realistic paintings. More specifically, Fig. 4a shows the brightfield image of a sample overpainted with an Ultramarine Blue layer, whereas Fig. 4b depicts the underlying pencil sketch before the application of the paint. Fig. 4c corresponds to a high contrast PA reconstruction of the underdrawing, as a result of the selective absorption of infrared radiation by the graphite deposition regions rather than the overlying paint layer. Our diagnostic approach was further compared with infrared imaging (Fig. 4d) within a similar optical spectral band (central wavelength: 1050 nm, FWHM: 25 nm), which constitutes the state of the art method for underdrawings visualization [12]. As it is clear from the respective figures, the two imaging methods provide highly comparable results for the case of Ultramarine Blue paint in terms of spatial resolution and contrast specificity. Similar data are additionally presented for a Chromium Green painting sample (Fig. 4e–h), validating once more the capabilities of non-contact and non-invasive PA diagnosis as regards to the accurate underdrawings detection. Nevertheless, the non-contact PA system has the potential to reveal hidden features in paintings for cases that the conventional infrared imaging fails as a result of excessive optical scattering and absorption of the overlying paint in the near infrared. Fig. 4i depicts a painting sample covered with Vermillion red paint, whereas Fig. 4j shows the respective pencil sketch prior overpainting. As it is clear from Fig. 4k, PA imaging has been able to recover successfully the hidden underdrawing, with reduced contrast though, due to the strong optical absorption background of the paint. In contrast to these results, the infrared image recorded within a similar optical excitation band

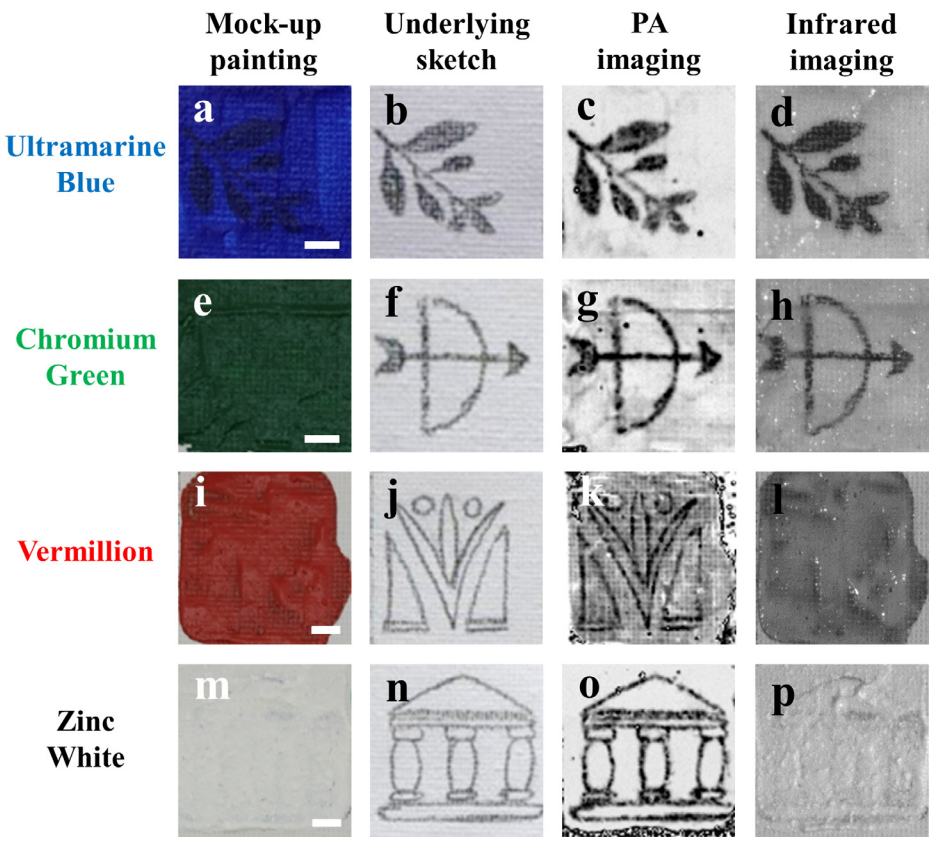

Fig. 4. Non-contact PA detection of hidden underdrawings for various samples covered with different test paints. (a) Brightfield view of a mock-up painting sample using an Ultramarine Blue paint layer. (b) Brightfield view of the underlying pencil sketch prior overpainting. (c) Recovered underdrawing pattern through PA imaging. (d) Near infrared optical image of the painting sample recorded at 1050 nm. Similar data are presented for Chromium Green (e–h), Vermillion (i–l) and Zinc White (m–p) paints. All scalebars are equal to 5 mm. (For interpretation of the references to colour in this figure legend, the reader is referred to the web version of this article.)

(Fig. 4l) could not provide any information regarding the underlying pencil sketch. A similar relative performance was also observed in the case of a Zinc White paint sample (Fig. 4m), with extremely high reflectivity and optical scattering properties. The hidden pencil sketch (Fig. 4n) was visualized with excellent contrast levels using PA imaging (Fig. 4o) due to the absence of any significant optical absorption background, as well as, the negligible attenuation/scattering of the generated acoustic waves during their transmission through the layer. Despite the minimum optical absorption, the respective infrared image (Fig. 4p) was once more unsuccessful to provide useful contrast of the pencil pattern, as a direct consequence of the extreme light diffusion occurring during the double-pass of infrared radiation in the paint layer.

4. Conclusions

In conclusion, we have demonstrated the highly promising potential of a non-contact and non-invasive PA imaging system integrating a spherically focused transducer as regards to the high contrast visualization of hidden features in paintings. By overcoming the restrictive requirements for a coupling medium in direct contact with the object, the developed apparatus could be employed for case studies involving the investigation of paintings with historical significance, considerably complementing the capabilities of existing methods for this purpose. Despite the fact that the overall performance of the developed apparatus is in general lower than typical PA imaging systems integrating immersion transducers, the provided sensitivity and spatial resolution have been proven to be sufficient for the faithful recovery of hidden features in a work of art. Since near infrared excitation radiation is heavily scattered on the canvas substrate prior its absorption by the paint layer, the local energy fluence is expected to be quite low to enable temperature changes that would induce any alterations in the painting materials [13]. Furthermore, due to the fact that most of the pigments contained in paint layers are generally transparent at 1064 nm, no photochemical modifications are expected to take place, even for relatively large energy fluences.

The current study has investigated cases of paintings where the hidden underdrawings are consisted of graphite. However, the proposed PA technique has the potential to image sketches drawn using other common carbon-based art media such as charcoal and carbon black paint, as has already been demonstrated by a previous study [6]. Given that PA signal amplitude is directly proportional to the optical absorption magnitude, the imaging contrast limitation is ultimately determined by the absorption coefficient difference between the overlying paint and the sketching material for the employed excitation wavelength. As a result, PA imaging is not expected to recover underdrawings well-hidden below high concentration carbon containing pigments due to the loss of useful imaging contrast. Nevertheless, as it has already been shown previously [6], PA detection performs significantly better than pure near infrared imaging in cases of dark paint layers containing up to 2% carbon pigment. Furthermore, a multispectral PA excitation approach combined with suitable spectral unmixing algorithms could enable a high sensitivity differentiation of absorbers presenting comparable absorption properties, in a similar manner to numerous biomedical imaging applications [3]. Finally, it should be noted that the developed experimental apparatus is limited to the imaging of relatively thin artworks such as the ones investigated in the current study. An epi-illumination geometry integrating laser excitation and PA detection on one side could be adopted in a future upgraded version of the proposed imaging system, providing universal diagnostic capabilities for art objects of arbitrary thickness and shape. Such a technological advancement combined with the effectiveness, the simplicity, the robustness and the relatively low cost features offered by non-invasive PA diagnosis, are anticipated to contribute in its wide adoption as a highly powerful tool regarding the in-depth investigation of various artworks.

Funding

This work was supported by Stavros Niarchos Foundation [ARCHERS]; POLITEIA II [MIS 5002478]; Skin-DOCtor [No 1778]; EU FP7 Marie Curie ITN OILTEBIA [PITN-GA-2012-317526]; H2020 Laserlab Europe [EC-GA 654148]; EU Community's H2020 IPERION CH Project [GA n. 654028]; and HELLAS CH [MIS 5002735].

Declaration of Competing Interest

None.

Appendix A. Supplementary material

Supplementary data to this article can be found online at https://doi.org/10.1016/j.ultras.2019.06.008.

References

[1] K. Trentelman, K. Janssens, G. van der Snickt, Y. Szafran, A.T. Woollett, Rembrandt's an old man in military costume: the underlying image re-examined, Appl. Phys. A 121 (3) (2015) 801–811, https://doi.org/10.1007/s00339-015-9426-3.

[2] Artnet News, Hidden Portrait Discovered Beneath the Surface of Picasso Painting, 2014. https://news.artnet.com/exhibitions/hidden-portrait-discovered-beneath-the-surface-of-picasso-painting-41747 (accessed 21 January 2019).

[3] J. Yao, L.V. Wang, Photoacoustic microscopy, Laser Photonics Rev. 7 (5) (2013) 758–778, https://doi.org/10.1002/lpor.201200060.

[4] M.I. Khan, G.J. Diebold, The photoacoustic effect generated by an isotropic solid sphere, Ultrasonics 33 (4) (1995) 265–269, https://doi.org/10.1016/0041-624X(95)00034-Z.

[5] M.I. Khan, G.J. Diebold, The photoacoustic effect generated by laser irradiation of an isotropic solid cylinder, Ultrasonics 34 (1) (1996) 19–24, https://doi.org/10.1016/0041-624X(95)00128-P.

[6] G.J. Tserevelakis, I. Vrouvaki, P. Siozos, K. Melessanaki, K. Hatzigiannakis, C. Fotakis, G. Zacharakis, Photoacoustic imaging reveals hidden underdrawings in paintings, Sci. Rep 7 (1) (2017), https://doi.org/10.1038/s41598-017-00873-7 art. no. 747.

[7] G.J. Tserevelakis, A. Dal Fovo, K. Melessanaki, R. Fontana, G. Zacharakis, Photoacoustic signal attenuation analysis for the assessment of thin layers thickness in paintings, J. Appl. Phys. 123 (12) (2018), https://doi.org/10.1063/1.5022749 art. no. 123102.

[8] G.J. Tserevelakis, M. Tsagkaraki, P. Siozos, G. Zacharakis, Uncovering the hidden content of layered documents by means of photoacoustic imaging, Strain 55 (2) (2019), https://doi.org/10.1111/str.12289 art. No. e12289.

[9] H. Liang, Advances in multispectral and hyperspectral imaging for archaeology and art conservation, Appl. Phys. A 106 (2) (2012) 309–323, https://doi.org/10.1007/s00339-011-6689-1.

[10] P. Targowski, M. Iwanicka, Optical coherence tomography: Its role in the non-invasive structural examination and conservation of cultural heritage objects – a review, Appl. Phys. A 106 (2) (2012) 265–277, https://doi.org/10.1007/s00339-011-6687-3.

[11] M. Schreiner, B. Frühmann, D. Jembrih-Simbürger, R. Linke, X-rays in art and archaeology: an overview, Powder Diffr. 19 (1) (2004) 3–11, https://doi.org/10.1154/1.1649963.

[12] A. Zacharopoulos, K. Hatzigiannakis, P. Karamaoynas, V.M. Papadakis, M. Andrianakis, K. Melessanaki, X. Zabulis, A method for the registration of spectral images of paintings and its evaluation, J. Cult. Herit. 29 (2018) 10–18, https://doi.org/10.1016/j.culher.2017.07.004.

[13] M. Popescu, L. Serban, M. Popescu, Thermo-indicating paint for damage warning, J. Therm. Anal. Calorim. 46 (1) (1996) 317–321, https://doi.org/10.1007/BF01979971.